The Hydration Structure of NO_3^- in Concentrated Aqueous Sodium Nitrate Solutions

Yasuo KAMEDA,* Hiroki SAITOH, and Osamu UEMURA
Department of Chemistry, Faculty of Science, Yamagata University, Kojirakawa-machi 1-4-12, Yamagata 990
(Received January 12, 1993)

Time-of-flight neutron diffraction measurements have been carried out on 10 mol% $NaNO_3$ solution in D_2O. The isotopic substitution technique was applied to nitrogen atoms in the solution in order to determine both hydration structure around the nitrate ion, NO_3^-, and intramolecular geometry of NO_3^- in the aqueous solution. It has become apparent that there exist 5.0±0.5 water molecules coordinated to NO_3^- with the intermolecular distance $r(N\cdots D)$ =2.80 Å. The intramolecular bond distance and the root mean square amplitude in NO_3^- have been determined to be r_{NO}=1.253±0.006 Å and l_{NO}=0.058±0.008 Å, respectively.

It has been a matter of interest for a long time to elucidate the hydration structure of nitrate ion, NO_3^-, and the solvation effect on the intermolecular structure of water molecules in the aqueous solution. This nitrate ion has been classified as the "order-destroying anion" in hydrogen-bonded liquid water, reflecting its large effective ionic radius and relatively small charge.[1] The hydration number of NO_3^- in an aqueous $NaNO_3$ solution has been reported to be 0.5 from NMR measurements.[2] This indicates that water molecules directly coordinated to NO_3^- is extremely slight in the aqueous solution. A recent double-difference infrared spectroscopic study on a $Ni(NO_3)_2$ solution[3] has exhibited that an uncoupled O–D stretching vibrational band of HDO molecules neighboring with NO_3^- is considerably broadened, which implies a wide distribution of $NO_3^-\cdots$water distances. The hydration number of NO_3^- has been estimated to be 3.7 in this spectroscopic study, which disagrees with the NMR results.

The hydration structure of NO_3^- has more directly been investigated by X-ray diffraction for concentrated NH_4NO_3[4] and $NaNO_3$[5] aqueous solutions. The intermolecular distances and the root mean square displacements have been obtained by a least squares fit of the measured X-ray interference functions to the theoretical ones on the basis of a short-range structure model around the constituent ions. The intermolecular distance between the oxygen atoms within NO_3^- and the neighboring water molecules reported in these diffraction measurements is 2.9 Å for both solutions. This value suggests that NO_3^- and neighboring water molecules are mutually hydrogen-bonded in the aqueous solution. However, it is considerably difficult to deduce the detailed hydration structure of NO_3^- from the X-ray diffraction data alone, because several interatomic correlations overlap in the range of the radial distance, $2<r<4$ Å, where the $NO_3^-\cdots H_2O$ correlation should be contained. In particular, the information on the orientational configuration between NO_3^- and the surrounding H_2O molecules cannot be given from the X-ray diffraction measurement owing to the extremely weak scattering power of hydrogen atoms.

Much clearer structural information has been supplied through a neutron diffraction study for 12.3 mol% $NaNO_3$ solution[6] applying the $^{14}N/^{15}N$ isotopic substitution technique. The distribution function around the nitrogen atom, $\overline{G}_N(r)$ obtained in this study, has proved that there exist five water molecules coordinated to NO_3^- as a total, both axially (r_{ND}=2.05 Å) and radially (r_{ND}=2.65 Å), in the first hydration shell of this ion. The intermolecular distance, r_{ND}=2.05 Å, between the nitrogen atom and deuteron atoms axially coordinated is much shorter than the sum of van der Waals radii of both atoms (2.8 Å). This result evidenced that the strong hydrogen bond between N and D atoms is formed in the aqueous solution. However, the $\overline{G}_N(r)$ obtained for other aqueous solutions, i.e., concentrated ND_4NO_3[7,8] and $LiNO_3$[9] solutions gives no indication of the pronounced peak around $r=2$ Å. After all, it seems that there still remain some problems on the hydration structure of NO_3^- in the aqueous solution.

Another question emerges on the intramolecular N–O bond length of NO_3^- in the aqueous solution. Recent results of time-of-flight (TOF) neutron diffraction studies for some molten alkali metal nitrates have shown that the intramolecular N–O distance is cation-independent and has the value of r_{NO}=1.251 Å.[10,11] This value in the molten state is 0.03 Å larger than that in the crystalline state reported by X-ray diffraction of a single $NaNO_3$ crystal (r_{NO}=1.218 Å).[12] On the other hand, Raman spectroscopic studies have indicated that the vibrational frequency associated with the symmetrical stretching mode of NO_3^- has only a small shift (at most ca. 20 cm^{-1}) among crystalline[13] and molten states,[14] and aqueous solutions.[15] This closeness of the vibrational frequency in different phases is therefore in conflict with the diffraction data.

The TOF neutron diffraction with the isotopic substitution of $^{14}N/^{15}N$ is one of the most suitable experimental methods to solve these problems. In this paper we report the result of TOF neutron diffraction measurements for 10 mol% $NaNO_3$ solutions in D_2O including two kinds of nitrogen isotopes. We will give direct experimental information both on the hydration structure around NO_3^- and on the intramolecular structure of this anion in the aqueous solution.

Experimental

Materials. Isotopically enriched sample $Na^{15}NO_3$ (99.0% ^{15}N, CIL Inc.) and natural $NaNO_3$ (99.6% ^{14}N; natural abundance) of reagent grade, both dried in vacuo, were dissolved into D_2O (99.8% D, Merck Inc.) to prepare two kinds of 10 mol% $NaNO_3$ aqueous solutions with different isotopic compositions of the N atoms. Isotopic compositions and mean scattering lengths of the N atoms in the solutions are listed up in Table 1, repectively. These solutions were sealed into cylindrical quartz cells (8 mm in inner diameter and 0.4 mm in thickness).

Neutron Diffraction Measurement. The TOF neutron diffraction measurement was carried out at 25 °C using the HIT spectrometer[16] installed at the pulsed spallation neutron source (KENS) in National Laboratory for High Energy Physics, Tsukuba, Japan. Scattered neutrons were detected by ^3He counters located at respective scattering angles of 2θ=8, 14, 25, 32, 44, 91, and 150°. The data accumulation time was ca. 8 h for both samples. Measurements were made in advance for an empty cell, background and a vanadium rod which has the same dimension as the sample.

Data Reduction. The measured scattering data were corrected for the background intensity, the absorption of both sample and cell,[17] the multiple[18] and the incoherent scatterings. The obtained count rate for the sample was converted to the absolute scale by the use of scattering intensity from the vanadium rod. The first-order difference function,[19] $\Delta_N(Q)$, was determined from the numerical difference in the normalized scattering cross section between the two solutions. The inelasticity effect, arising from the self scattering contribution of deuterium atoms, is expected to be canceled out in the term of $\Delta_N(Q)$ through the subtraction of two scattering data sets in which the identical inelasticity distortion is individually included. After all, it was recognized in the present work that the inelasticity effect is negligibly small in $\Delta_N(Q)$ even at the large scattering angle such as 2θ=91°.[19,20] Since $\Delta_N(Q)$s obtained experimentally at various scattering angles, 2θ=14—91°, agree well each other within the statistical errors, it was allowed to combine the data of the scattering angles from 2θ=14 to 91°. The whole $\Delta_N(Q)$ for the 10 mol% $NaNO_3$ aqueous solution was determined in this way as in Fig. 1a.

$\Delta_N(Q)$ can be represented by the linear combination of the four partial structure factors including contributions concerning the nitrogen atom, i.e.,

$$\Delta_N(Q) = A[a_{NO}(Q) - 1] + B[a_{ND}(Q) - 1] + C[a_{NNa}(Q) - 1] + D[a_{NN}(Q) - 1], \quad (1)$$

where

$$A = 2c_N c_O b_O (b_{14N} - b_{15N})$$
$$B = 2c_N c_D b_D (b_{14N} - b_{15N})$$
$$C = 2c_N c_{Na} b_{Na} (b_{14N} - b_{15N})$$
$$D = c_N{}^2 (b_{14N}{}^2 - b_{15N}{}^2),$$

and c_i is the number of i-th atom in the stoichiometric unit $(NaNO_3)_{0.1}(D_2O)_{0.9}$. The value of weighting factors A, B, C, and D is numerically listed up in Table 2.

The Fourier transform of $\Delta_N(Q)$ yields the distribution function around the nitrogen atom, $\overline{G}_N(r)$,

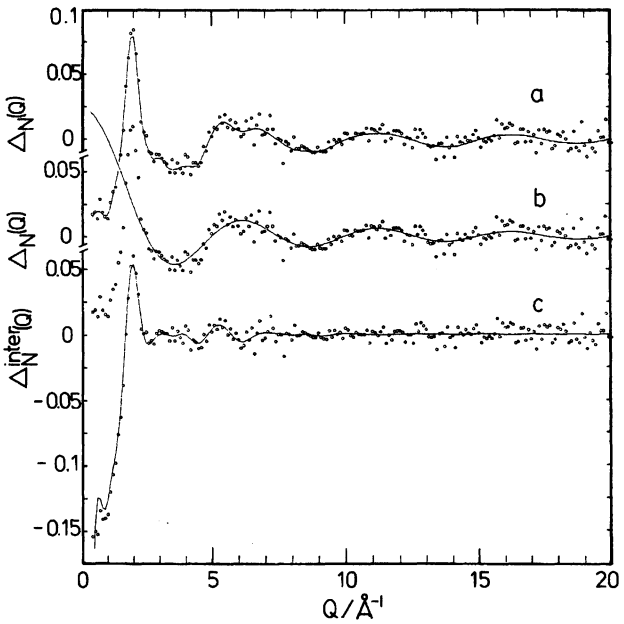

Fig. 1. a) Circles: The observed difference function, $\Delta_N(Q)$, for 10 mol% $NaNO_3$ solution in D_2O. The solid line: Smoothed $\Delta_N(Q)$ used for Fourier transform (Fig. 2a). b) Circles: The observed $\Delta_N(Q)$. The solid line: The intramolecular N–O contribution, $I^{intra}(Q)$. c) Circles: The intermolecular contribution, $\Delta_N^{inter}(Q)$. The solid line: The back Fourier transform of $\overline{G}_N^{inter}(r)$ shown in Fig. 2b.

$$\begin{aligned}\bar{G}_N(r) &= 1 + (A + B + C + D)^{-1}(2\pi^2\rho r)^{-1} \\ &\quad \times \int_0^{Q_{max}} Q\Delta_N(Q)\sin(Qr)dQ \\ &= [Ag_{NO}(r) + Bg_{ND}(r) + Cg_{NNa}(r) + Dg_{NN}(r)] \\ &\quad \times (A + B + C + D)^{-1}, \end{aligned} \quad (2)$$

which is given in Fig. 2a. $\overline{G}_N(r)$ is mainly dominated by $g_{NO}(r)$ and $g_{ND}(r)$ terms since contribution factors, A and B, are much larger than those, C and D, as indicated in Table 2.

Results and Discussion

The observed $\Delta_N(Q)$, shown in Fig. 1a, has a dominant first peak at $Q \simeq 2$ Å^{-1}, partly splitted second peak at $Q \simeq 6$ Å^{-1} and periodic oscillational structure at the higher-Q side. These features in the present $\Delta_N(Q)$ are in agreement with those reported previously by Neilson and Enderby.[6] Figure 2a gives the distribution function around the nitrogen atom, $\overline{G}_N(r)$, obtained by the Fourier transform of the solid line in Fig. 1a. The upper limit of the integral, Q_{max}, was set to be 20.0 Å^{-1}. The first peak at r=1.25 Å in $\overline{G}_N(r)$ can be assigned to the intramolecular N–O interaction in NO_3^-. Termination ripples on the Fourier integration, caused by the set-up of finite upper limit Q_{max}=20.0 Å^{-1}, appear around the first peak. The intramolecular N–O correlation in the Q-space, $I^{intra}(Q)$, can be theoretically described as follows,

Table 1. The Isotopic Compositions and Mean Scattering Lengths b_N of Nitrogen Atoms, Mean Scattering and Absorption Cross Sections and the Number Densities Scaled in the Stoichiometric Unit $(NaNO_3)_{0.1}(D_2O)_{0.9}$, σ_s, σ_a, and ρ, Respectively, for the Samples Used in This Study

Samples	$^{14}N/\%$	$^{15}N/\%$	$b_N/10^{-12}$ cm	σ_s/barns	σ_a/barns[a)]	$\rho/Å^{-3}$
$Na^{14}NO_3$	99.6	0.4	0.936	20.552	0.245	0.0308
$Na^{15}NO_3$	1.0	99.0	0.649	19.932	0.055	

a) For the incident neutron wavelength of 1.8 Å.

Table 2. Values of the Coefficients of $a_{ij}(Q)$ in Eq. 1

A/barns	B/barns	C/barns	D/barns
0.0403	0.0694	0.0021	0.0046

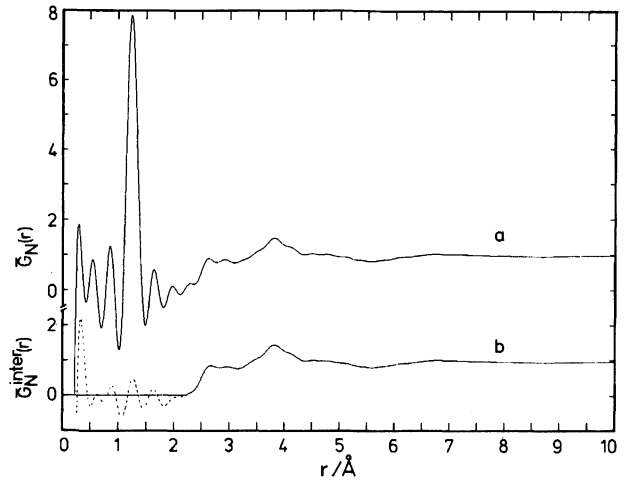

Fig. 2. a) The total and b) intermolecular distribution function around the nitrogen atom, $\overline{G}_N(r)$ and $\overline{G}_N^{inter}(r)$, truncated at $Q_{max}=20.0$ Å^{-1}, for 10 mol% $NaNO_3$ solution in D_2O.

$$I^{intra}(Q) = 2c_N n_{NO} b_O (b_{14N} - b_{15N}) \times \exp(-l_{NO}{}^2 Q^2/2) \frac{\sin Qr_{NO}}{Qr_{NO}}, \quad (3)$$

where n_{NO} is the coordination number of oxygen atoms around the nitrogen atom, and l_{NO} and r_{NO} denote the root mean square amplitude and internuclear distance of the N–O bond, respectively. Parameters, n_{NO}, l_{NO}, and r_{NO} in Eq. 3 were determined to be 3.2±0.3, 0.058±0.008 Å, and 1.253±0.006 Å, respectively, from a least-squares fitting in the range with $7<Q<20$ Å^{-1} between Eq. 3 and the observed $\Delta_N(Q)$. The fitting procedure was performed using the SALS program.[21)] The closeness of the magnitude of n_{NO} to the expected value (three) proves the validity of the present data corrections and normalization procedure. The value of intramolecular distance, r_{NO}, obtained is in complete agreement with $r_{NO}=1.25$ Å reported previously in TOF neutron[10,11,22)] and X-ray diffraction[23,24)] studies for some molten alkali nitrates. The result that the intramolecular structure of NO_3^- in the aqueous solution is the same as that in the molten state is also supported by spectroscopic studies.[13—15)] On the other hand, the value of $r_{NO}=1.218\pm0.004$ Å, reported by the X-ray diffraction study for a $NaNO_3$ single crystal,[12)] is 0.03 Å shorter than that obtained in the aqueous solution or in the molten state. If this were valid, one might expect that a marked difference in vibrational frequency of the symmetrical stretching mode for NO_3^- is present between the crystalline and solution states. However, the difference in this frequency has been observed to be at most ca. 20 cm^{-1}.[13—15)] The reason for this discrepancy mentioned above are still less clear at present.

The Fourier transform of the difference function at Q-space obtained by subtracting the theoretical $I^{intra}(Q)$ from observed $\Delta_N(Q)$ (Figs. 1b and 1c) provides the intermolecular distribution function, $\overline{G}_N^{inter}(r)$ (Fig. 2b), in which unphysical termination ripples below $r=2$ Å are much reduced. The structural components appearing at $r>2$ Å in $\overline{G}_N(r)$ remain unchanged after removing the intramolecular N–O contribution. Then, these components is considered to denote a real intermolecular structure. The overall feature of the present $\overline{G}_N(r)$ containing a broadened peak at $r=3.8$ Å with unresolved shoulder around 2.8 Å is very similar to the $\overline{G}_N(r)$ reported for other concentrated aqueous solutions such as $LiNO_3$[9)] and ND_4NO_3[7)] solutions by the first-order difference method of the neutron diffraction experiments; this result suggests little effect of the counter-cation on the hydration structure of NO_3^-. However, the nearest neighbor N···D peak at $r=2.05$ Å, reported previously for 12.3 mol% $NaNO_3$ solution ($Q_{max}=10.2$ Å^{-1}),[6)] is not observed in the present $\overline{G}_N(r)$. In order to discuss this disagreement, we transformed the observed $\Delta_N(Q)$ to $\overline{G}_N(r)$ with truncating at various upper limits, Q_{max}, the result of which is represented in Fig. 3. With decreasing value of Q_{max}, the height of the intramolecular N–O peak decreases while its peak width increases. In addition, the position of the N–O peak exhibits a systematic shift toward the lower values of r with decreasing Q_{max}: $r_{NO}=1.22$ Å for $Q_{max}=10.0$ Å^{-1} and 1.19 Å for $Q_{max}=7.4$ Å^{-1}. The peak position of 1.25 Å in $\overline{G}_N(r)$ truncated at $Q_{max}=20.0$ Å^{-1} agrees well with the intramolecular N–O distance obtained by the least-squares fitting to $\Delta_N(Q)$. The value of r_{NO}, 1.22 Å, in $\overline{G}_N(r)$ truncated at $Q_{max}=10.0$ Å^{-1} corresponds to that reported in the previous work by Neilson and

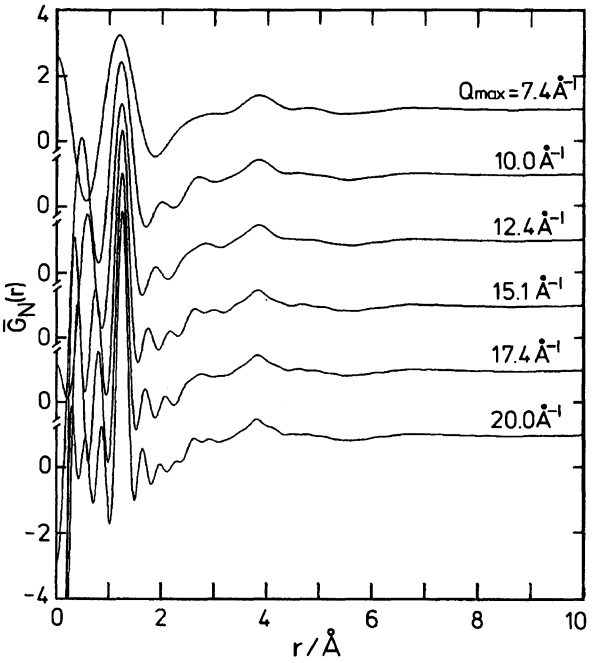

Fig. 3. The effect of different truncations of Q_{max} on the $\overline{G}_N(r)$ for 10 mol% $NaNO_3$ solution in D_2O.

Enderby ($r_{NO}=1.23\pm0.02$ Å at $Q_{max}=10.2$ Å^{-1}[6]).

Termination ripples around the N–O peak also indicate a systematic change in their period. The ghost maxima arising from the termination effect should appear in due order at distances from the main peak, $\Delta r\simeq\pm4\pi/2Q_{max}$, $\simeq\pm9\pi/2Q_{max}$, and so on.[25] Thus, the positions of ghost maxima at higher side will be $r=2.04$ and 2.66 Å in the present case of $r_{NO}=1.25$ Å and $Q_{max}=10.0$ Å^{-1}. This result corresponds well to positions of ghost maxima in present $\overline{G}_N(r)$ for $Q_{max}=10.0$ Å^{-1} as seen in Fig. 3. In the previous work for $Q_{max}=10.2$ Å^{-1} by Neilson and Enderby, they have assigned the peaks at $r=2.05$ and 2.65 Å in $\overline{G}_N(r)$ to the nearest neighbor N···D and N···O distances, respectively.[6] However, it is possible from the above discussion that substantial termination ripples are superimposed on their $\overline{G}_N(r)$ because of lower termination limit Q_{max}. In contrast, the termination effect contained in present $\overline{G}_N^{inter}(r)$ can be much smaller since $Q_{max}=20.0$ Å^{-1} was used and the intramolecular N–O contribution has been eliminated.

The broadened shape of $\overline{G}_N^{inter}(r)$ in Fig. 2b seems to represent the weak hydration nature of NO_3^-. Nevertheless, the features appearing at $r\simeq2.8$ and $r\simeq3.8$ Å in $\overline{G}_N^{inter}(r)$ indicate the existence of a preferred orientation between NO_3^- and the neighboring water molecules in the solution. According to the model structure for NO_3^- hydration proposed from X-ray diffraction results,[4,5] in which six water molecules are hydrogen-bonded with the oxygen atoms of NO_3^- in the first hydration shell, the feature at $r\sim2.8$ Å in $\overline{G}_N^{inter}(r)$, although poorly resolved, can be ascribed to the nearest neighbor N···D distance. The coordination number, n_{ND}, is tentatively derived from the following integral,

$$n_{ND} = \frac{A+B+C+D}{B}\int_{2.21}^{3.15} 4\pi c_D \rho r^2 \bar{G}_N^{inter}(r)dr = 5.0\pm0.5, \quad (4)$$

where the local minimum in $\overline{G}_N^{inter}(r)$ curve was taken as the upper limit of the integral. The error in n_{ND} mainly arises from the uncertainty in the overall normalization constant for the observed $\Delta_N(Q)$, which is nearly 10% judging from the error in the intramolecular coordination number $n_{NO}=3.2\pm0.3$ within NO_3^-. The value of n_{ND} obtained in the present study is roughly regarded as the hydration number, $n(NO_3^-\cdots H_2O)=6$, reported in the X-ray diffraction studies.[4,5] Then, the hydration structure around NO_3^- can be characterized by the following local configuration; one of hydrogen atoms of each water molecule within the first hydration shell is facing the oxygen atom of NO_3^- as illustrated in Fig. 4. The peak located around 3.8 Å in $\overline{G}_N^{inter}(r)$ can reasonably be identified with the intermolecular N···O_w. In addition, it is probable that N···D_2 interactions are absorbed in this peak. On the basis of this local structure model around NO_3^-, the structural parameters concerning the nearest neighbor N···D_2O contribution can be estimated using the present $r\overline{G}_N^{inter}(r)$ curve (Fig. 4). The nearest neighbor N···D_1, N···O_w and N···D_2 interactions have been described by their Gaussians. Further, the coordination number for respective peaks was taken to be 5.0. In this result, the peak position r(N···D_1) =2.8 Å and full width at half maximum w(N···D_1) =0.6 Å, were determined by a Gaussian fitting to the experimental $r\overline{G}_N^{inter}(r)$ within the range of $r<2.8$ Å (peak-a in Fig. 4). The parameters for N···O_w and N···D_2 contributions were also obtained to be r(N···O_w) =3.78 Å and w(N···O_w) =0.6

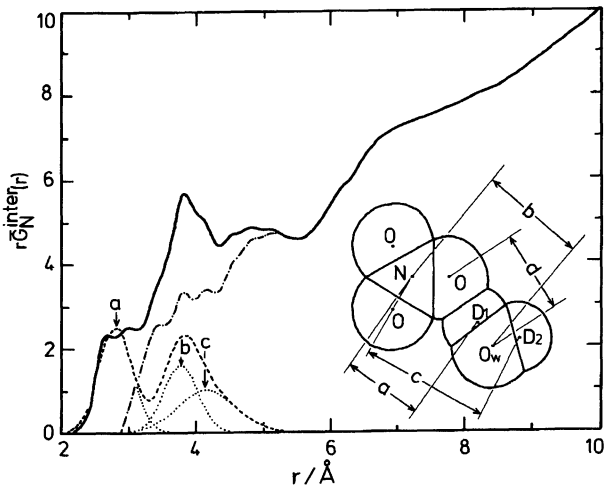

Fig. 4. A possible decomposition of the $r\overline{G}_N^{inter}(r)$ curve into the contributions from the nearest neighbor interactions N···D_1 (a), N···O_w (b) and N···D_2 (c).

Å (peak-b), $r(N\cdots D_2)$ =4.16 Å and $w(N\cdots D_2)$ =1.0 Å (peak-c) through the Gaussian fittings to $r\overline{G}_N^{inter}(r)$ in the range of $r<5$ Å. These parameters correspond well to the intermolecular distance $r(O\cdots O_w)$ =2.9 Å[5] previously reported (denoted by d in Fig. 4) and molecular geometries known for NO_3^- and D_2O.[26] Therefore, the prominent features in the experimental $r\overline{G}_N^{inter}(r)$ below $r\simeq 4$ Å are satisfactorily described by the present model for the nearest neighbor $NO_3^-\cdots D_2O$ correlation. Since the integral over the wide range of $2.21<r<4.38$ Å in $\overline{G}_N^{inter}$ is given as a total 9.8 water molecules, it appears that nearly a half of the water molecules in this r region is present in the well defined hydration geometry around NO_3^-.

The present result on the hydration structure of NO_3^- in aqueous 10 mol% $NaNO_3$ solution can be compared with our previous one of aqueous 10 mol% $NaNO_2$ solution,[27] in which experimental procedure (TOF neutron diffraction) and data treatment were all identical to those in the present work. $\overline{G}_N^{inter}(r)$ functions for both solutions exhibit a similar weak hydration behavior, such as poorly resolved nearest neighbor N···D and N···O peaks. However, a significant difference can be seen for the intermolecular peak positions. For example, the nearest neighbor N···D distance, corresponding to the first-peak position in $\overline{G}_N^{inter}(r)$, is 2.8 Å, for $NaNO_3$ solution, whereas, 2.7 Å for $NaNO_2$ solution. The nearest neighbor N···O distance for hydrated NO_3^- is nearly 0.3 Å longer than that for hydrated NO_2^-. These differences may be considered to come from the difference in the hydration geometry rater than that in the chemical property between NO_3^- and NO_2^-. However, it should be essential that partial pair distribution functions, $g_{ND}(r)$ and $g_{NO}(r)$, are separately obtained, to discuss more fully the difference on the hydration structure between both ions. This requires further diffraction experiments which involve not only the $^{14}N/^{15}N$ isotopic substitution technique but also H/D one, which will be a near-future subject.

We would like to acknowledge the member of HIT group during the course of diffraction measurements. All calculations were carried out with the ACOS 3600 computer at the computing Center of Yamagata University.

References

1) G. R. Choppin and K. Buijs, *J. Chem. Phys.*, **39**, 2042 (1963).
2) B. F. J. Vorgin, P. S. Knapp, W. L. Flint, A. Anton, G. Highberger, and R. Minowski, *J. Chem. Phys.*, **54**, 178 (1971).
3) P-Å. Bergström, J. Lindgren, and O. Kristiansson, *J. Phys. Chem.*, **95**, 8575 (1991).
4) R. Caminiti, G. Licheri, G. Piccaluga, and G. Pinna, *J. Chem. Phys.*, **68**, 1967 (1978).
5) R. Caminiti, G. Licheri, G. Paschina, and G. Pinna, *J. Chem. Phys.*, **72**, 4522 (1980).
6) G. W. Neilson and J. E. Enderby, *J. Phys. C: Solid State Phys.*, **15**, 2347 (1982).
7) P. A. M. Walker, D. G. Lawrence, G. W. Neilson, and J. Cooper, *J. Chem. Soc., Faraday Trans. 1*, **85**, 1365 (1989).
8) A. K. Adya and G. W. Neilson, *J. Chem. Soc., Faraday Trans. 1*, **87**, 279 (1991).
9) T. Yamaguchi, S. Tanaka, H. Wakita, and M. Misawa, "KENS REPORT-VIII," (1991), p. 90.
10) T. Yamaguchi, Y. Tamura, I. Okada, H. Ohtaki, M. Misawa, and N. Watanabe, *Z. Naturforsch*, **40a**, 490 (1985).
11) Y. Kameda, S. Kotani, and K. Ichikawa, *Mol. Phys.*, **75**, 1 (1992).
12) R. L. Sass, R. Vidale, and J. Donohue, *Acta Crystallogr.*, **10**, 567 (1957).
13) S. C. Wait, A. T. Ward, and G. J. Jantz, *J. Chem. Phys.*, **45**, 133 (1966).
14) D. W. James and W. H. Leong, *J. Chem. Phys.*, **51**, 640 (1969).
15) D. E. Irish and A. R. Davis, *Can. J. Chem.*, **46**, 943 (1968).
16) N. Watanabe, T. Fukunaga, T. Shinohe, K. Yamada, and T. Mizoguchi, "Proc. 4th International Collaboration on Advanced Neutron Sources (ICANS-IV) KEK, Tsukuba" ed by Y. Ishikawa et al. (1981), p.539.
17) H. H. Paalman and C. J. Pings, *J. Appl. Phys.*, **33**, 2635 (1962).
18) I. A. Blech and B. L. Averbach, *Phys. Rev.*, **137**, 1113 (1965).
19) A. K. Soper, G. W. Neilson, J. E. Enderby, and R. A. Howe, *J. Phys. C: Solid State Phys.*, **10**, 1793 (1977).
20) K. Ichikawa, Y. Kameda, T. Matsumoto, and M. Misawa, *J. Phys. C: Solid State Phys.*, **17**, L725 (1984).
21) T. Nakagawa and Y. Oyanagi, "Recent Developments in Statistical Inference and Data Analysis," ed by K. Matushita, North-Holland (1980), p. 221.
22) K. Suzuki and K. Fukushima, *Z. Naturforsch*, **32a**, 1438 (1977).
23) H. Ohno and K. Furukawa, *J. Chem. Soc., Faraday Trans. 1*, **74**, 297 (1978).
24) A. K. Adya, R. Takagi, K. Kawamura, and M. Mikami, *Mol. Phys.*, **62**, 227 (1987).
25) Y. Waseda, "The Structure of Non-Crystalline Materials," MacGraw-Hill (1980), p. 34.
26) Y. Kameda and O. Uemura, *Bull. Chem. Soc. Jpn.*, **65**, 2021 (1992).
27) Y. Kameda, H. Arakawa, K. Hangai, and O. Uemura, *Bull. Chem. Soc. Jpn.*, **65**, 2154 (1992).